# Hormonal control of the renal immune response and antibacterial host defense by arginine vasopressin

Cécilia Chassin,[1,2] Mathias W. Hornef,[3] Marcelle Bens,[1,2] Michael Lotz,[3] Jean-Michel Goujon,[4] Sophie Vimont,[5,7] Guillaume Arlet,[5,7] Alexandre Hertig,[6,7] Eric Rondeau,[6,7] and Alain Vandewalle[1,2]

[1]Institut National de la Santé et de la Recherche Médicale (INSERM), U773, Centre de Recherche Biomédicale Bichat-Beaujon (CRB3), BP 416, 75018 Paris, France
[2]Université Paris 7–Denis Diderot, site Bichat, Paris, 75870 Paris, France
[3]Institute for Medical Microbiology and Hygiene, University of Freiburg, 79104 Freiburg, Germany
[4]Service d'Anatomie et Cytologie Pathologiques, Centre Hospitalier Universitaire de Poitiers, Université de Poitiers, 86021 Poitiers, France
[5]Service de Bactériologie and [6]INSERM, U702, Hôpital Tenon, 75970 Paris, France
[7]Université Paris 6–Pierre et Marie Curie, site St. Antoine, Paris, 75571 Paris, France

CORRESPONDENCE
Alain Vandewalle:
vandewal@bichat.inserm.fr

Abbreviations used: AVP, arginine vasopressin; cAMP, cyclic AMP; CCD, cortical collecting duct; CFTR, cystic fibrosis transmembrane conductance regulator; dDAVP, deamino-8-D-AVP; ENaC, epithelial sodium channel; Gly, glybenclamide; ICAM, intracellular adhesion molecule; MIP-2, macrophage inflammatory protein 2; MPO, myeloperoxidase; MyD88. myeloid differentiation factor 88; NPPB, 5-nitro-2(3phenylpropyl-amino) benzoate; PKA, protein kinase A; PP1 and PP2A, protein phosphatase 1 and 2A, respectively; RANTES, regulated on activation, normal T cell expressed and secreted; Ser/ Thr, serine/threonine; siRNA, small-interfering RNA; TLR, Toll-like receptor; UPEC, uropathogenic *Escherichia coli*; UTI, urinary tract infection; V2R, V2 receptor.

**Ascending urinary tract infection (UTI) and pyelonephritis caused by uropathogenic *Escherichia coli* (UPEC) are very common infections that can cause severe kidney damage. Collecting duct cells, the site of hormonally regulated ion transport and water absorption controlled by vasopressin, are the preferential intrarenal site of bacterial adhesion and initiation of inflammatory response. We investigated the effect of the potent V2 receptor (V2R) agonist deamino-8-D-arginine vasopressin (dDAVP) on the activation of the innate immune response using established and primary cultured collecting duct cells and an experimental model of ascending UTI. dDAVP inhibited Toll-like receptor 4–mediated nuclear factor κB activation and chemokine secretion in a V2R-specific manner. The dDAVP-mediated suppression involved activation of protein phosphatase 2A and required an intact cystic fibrosis transmembrane conductance regulator Cl⁻ channel. In vivo infusion of dDAVP induced a marked fall in proinflammatory mediators and neutrophil recruitment, and a dramatic rise in the renal bacterial burden in mice inoculated with UPECs. Conversely, administration of the V2R antagonist SR121463B to UPEC–infected mice stimulated both the local innate response and the antibacterial host defense. These findings evidenced a novel hormonal regulation of innate immune cellular activation and demonstrate that dDAVP is a potent modulator of microbial–induced inflammation in the kidney.**

Urinary tract infection (UTI) and pyelonephritis, which are usually caused by uropathogenic *Escherichia coli* (UPEC), are common infectious diseases that constitute a notable risk factor for the development of renal insufficiency in children, young adults and renal transplanted patients (1–3). Toll-like receptor (TLR) 4, which recognizes LPS, an obligate constituent of the outer membrane of all Gram-negative bacteria, plays a central role in initiating the antibacterial host response: LPS-defective (*Lps^d*) C3H/HeJ mice exhibiting a loss-of-function mutation in the *Tlr4* gene are unresponsive to LPS (4) and

fail to clear Gram-negative bacteria colonizing the lower urinary tract and kidneys (5). Using an experimental mouse model of ascending pyelonephritis, we have shown that when UPECs invade the kidneys, they bind specifically to the apical surface of collecting duct (CD) cells (6) and induce a potent proinflammatory response via distinct TLR4-dependent and –independent signaling pathways (6, 7). These findings indicate that, like bladder epithelial cells (8), epithelial cells from the collecting duct (which is the first tubule segment to encounter ascending bacteria), together with bone marrow–derived cells (8, 9), play a key role in initiating an innate immune response in the kidney.

The online version of this article contains supplemental material.

Collecting duct cells are a major site of the reabsorption of water and of NaCl from the primitive urine. These processes are tightly regulated by hormones such as arginine vasopressin (AVP), a neuropeptide secreted into the systemic bloodstream by hypothalamic neurons, which binds to V2 receptors (V2Rs) coupled to adenylyl cyclase and stimulates the cyclic AMP (cAMP)–protein kinase A (PKA) signaling pathway. This boosts the reabsorption of water by increasing the permeability of the apical membranes of the collecting duct principal cells (10). AVP also stimulates the reabsorption of NaCl mediated by the epithelial sodium channel (ENaC) and activates the cAMP-sensitive cystic fibrosis transmembrane conductance regulator (CFTR) Cl⁻ conductance in cultured renal collecting duct cells (11–13). Children with pyelonephritis exhibit increased levels of circulating AVP and develop polyuria with urinary concentrating defect, probably related to acute renal interstitial inflammation (14–16). However, this does not exclude that vasopressin may produce unexpected biological effects on renal cells independently of its antidiuretic action. As a matter of fact, the mechanisms involved in the interplay between AVP and renal inflammatory responses caused by LPS or UPECs are still poorly understood. Previous studies have shown that increased cell cAMP levels inhibit the TNF-α–, LPS-, and IL-1β–stimulated expression of adhesion molecules and signaling molecules in a variety of cell types (17–20). AVP, via its stimulatory action on cell cAMP content, might therefore inhibit the activation of target cells (i.e., collecting duct cells) after bacterial colonization of the kidney. However, the effects of AVP on proinflammatory mediators and the upstream and downstream mechanisms of cAMP-mediated inhibition of cellular activation remain to be identified. The fact that UPECs preferentially adhere to AVP-sensitive collecting duct cells that are able to develop a potent inflammatory response (6) led us to hypothesize that AVP may influence the innate immune response and affect renal bacterial clearance. In the present study, we examine the effects of 1-deamino-8-D-AVP (dDAVP), a pure V2R agonist, on LPS recognition in immortalized cortical collecting duct (CCD) mpkCCD$_{cl4}$ cells that have retained the main properties of the parent collecting duct cells (11, 21) and their sensitivity to LPS (22). We carefully analyze the underlying molecular process and show that dDAVP inhibits LPS-mediated cell activation through a dephosphorylation process, which is mainly mediated by the serine/threonine (Ser/Thr) protein phosphatase 2A (PP2A). Using CCD cells dissected from homozygous *cftr*$^{m1unc}$ mice in which the *cftr* gene had been disrupted (23) and their wild-type counterparts, we further demonstrated the important role played by CFTR in this process. Using an experimental model of ascending UTI (4), we also provide in vivo demonstration of the relevance of the regulatory role of dDAVP in controlling renal inflammatory responses. Overall, our findings identify a novel AVP–CFTR–Ser/Thr PP2A regulatory pathway involved in controlling the intrarenal innate immune response to pyelonephritis caused by UPEC.

## RESULTS

### Renal collecting duct mpkCCD$_{cl4}$ cells express TLR4 and are sensitive to LPS

The identification of collecting duct cells as a preferential adhesion site for UPECs in an in vivo model of ascending UTI (6) led us to analyze the mechanisms of cell activation in a highly differentiated collecting duct cell line, mpkCCD$_{cl4}$, derived from collecting ducts microdissected from the kidney of a transgenic SVPK–Tag mouse harboring the large T antigen under the control of a truncated pyruvate kinase promoter fused to an SV40 enhancer (21). These cells formed confluent layers of epithelial-shaped cells, which in turn formed domes, a characteristic feature of layers of ion-transporting epithelial cells (Fig. S1, available at http://www.jem.org/cgi/content/full/jem.20071032/DC1). mpkCCD$_{cl4}$ cells expressed TLR4 as well as the accessory protein MD-2 and myeloid differentiation factor 88 (MyD88; Fig. S1). They also expressed the mRNA of CD14 (Fig. S1), indicating that mpkCCD$_{cl4}$ cells might autonomously produce CD14, rendering them independent of serum-derived soluble CD14. Western blotting using a specific polyclonal rabbit anti-TLR4 antiserum revealed a major protein band of the predicted size of ∼96 kD, which was not detected in the presence of an excess of the peptide used for immunization (Fig. 1 A). FACS analysis revealed predominantly intracellular staining of TLR4 (Fig. 1 B), and immunofluorescence studies showed that TLR4 was mainly concentrated in the perinuclear region of the cytoplasm (Fig. 1 C, top), where it colocalized with the Golgi marker CTR433 (Fig. 1 C, bottom) (24). These findings indicate that mpkCCD$_{cl4}$ cells express the LPS receptor complex TLR4–MD-2, which is mainly detected in the intracellular compartment (i.e., in the Golgi apparatus), as previously reported in pulmonary epithelial cells (25), endothelial cells (26), and intestinal epithelial m-IC$_{cl2}$ cells (27).

The recognition of LPS by TLR4 induces a cascade of events leading to activation of the nuclear transcription factor NF-κB signaling pathway and the subsequent production of chemokines and cytokines (28). IκB-α undergoes ubiquitination and proteasome-mediated degradation, leading to the release and nuclear translocation of the NF-κB subunit p65/RelA (29, 30). In mpkCCD$_{cl4}$ cells, LPS induced the nuclear translocation of NF-κB (Fig. 1 D, top). This nuclear redistribution was completely abolished after treatment with the specific NF-κB inhibitor SN50. LPS also induced a dose-dependent increase in luciferase activity in cells transiently transfected with a NF-κB luciferase reporter gene construct (Fig. 1 D, bottom). 50 ng/ml TNF-α, used as positive control, similarly induced a significant increase in luciferase activity. Finally, LPS induced dose- and time-dependent stimulation of the secretion of the chemokine macrophage inflammatory protein 2 (MIP-2; Fig. 1 E), which was very significantly reduced in the presence of SN50 or polymyxin B, a competitive inhibitor of LPS (not depicted). These results indicate that mpkCCD$_{cl4}$ cells provide a suitable in vitro cell system for analyzing regulatory mechanisms controlling TLR4-mediated cellular activation in renal collecting duct cells.
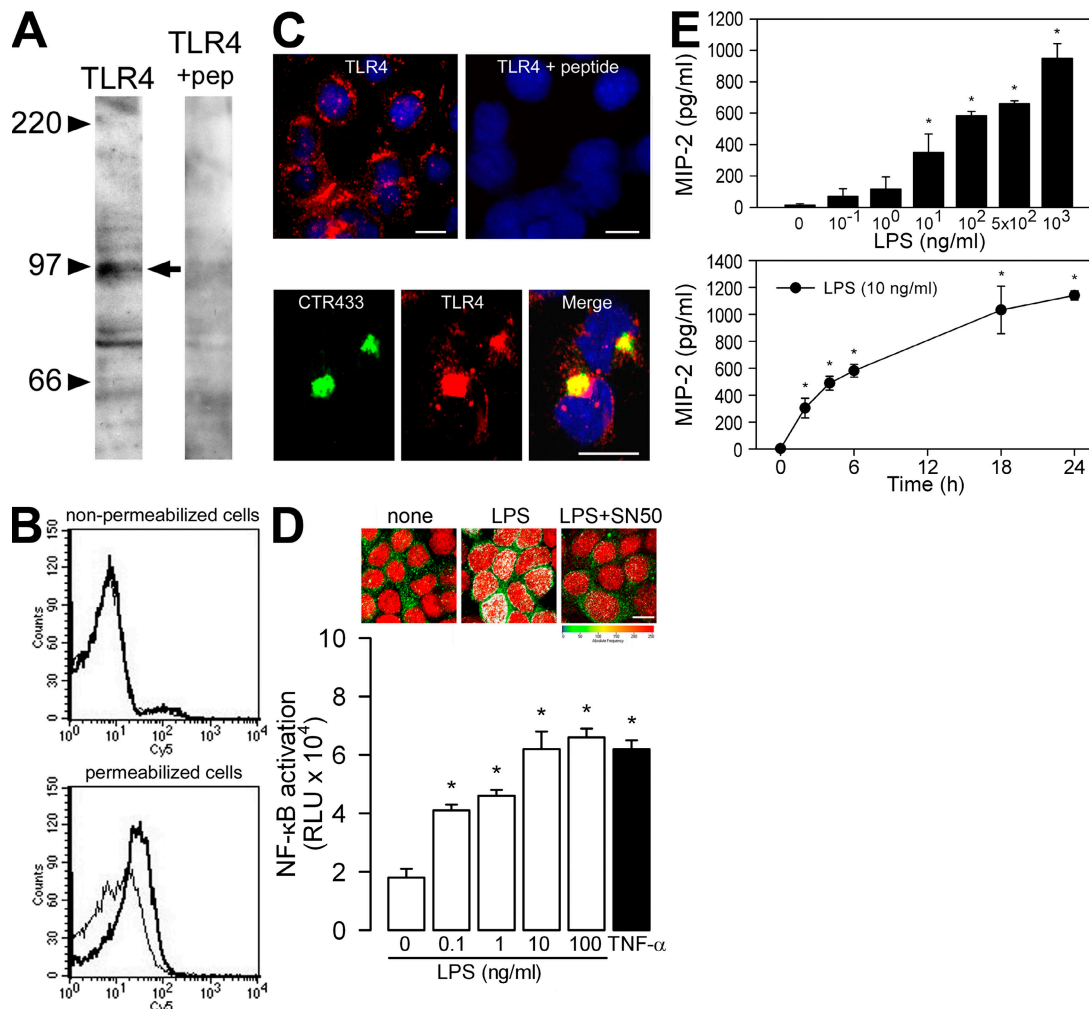
**Figure 1. TLR4 expression in CCD mpkCCD_{cl4} cells.** (A) Western blot analysis of mpkCCD_{cl4} cell lysates revealing a band of the predicted size (~96 kD; arrow) of TLR4, which was not detected in the presence of an excess of the peptide (+pep) used for immunization. (B) FACS analysis for TLR4 in nonpermeabilized and permeabilized cells. Nonbolded lines correspond to the isotype control. (C) Cellular immunolocalization of TLR4 performed with or without an excess of the peptide used for immunization (top), and colocalization of TLR4 with the Golgi apparatus marker CTR433 (bottom). Nuclei were counterstained with HOECHST 33258. Bars, 10 μm. (D, top) Nuclear translocation of NF-κB p65/RelA in cells stimulated with 10 ng/ml LPS in the presence or absence of 18 μM SN50 for 3 h. Bar, 10 μm. (bottom) Effects of rising concentrations of LPS and 50 ng/ml TNF-α on NF-κB activation in cells transfected with the NF-κB luciferase reporter. (E) Effects of rising concentrations of LPS and time dependency on the secretion of MIP-2. Values are means ± SE from four to seven experiments. *, P < 0.05 versus zero values.

## dDAVP inhibits LPS-dependent NF-κB activation and secretion of MIP-2 and TNF-α in renal collecting duct mpkCCD_{cl4} cells

Previous studies had demonstrated that AVP induces a rapid rise in cellular cAMP content and stimulates the reabsorption of NaCl and water by renal collecting duct cells (17–20). We investigated whether dDAVP could affect innate immune recognition of LPS in mpkCCD_{cl4} epithelial cells. Incubating cells with $10^{-8}$ M dDAVP alone or with LPS for 6 h induced a significant rise in cAMP as compared with untreated cells (Fig. 2 A). LPS induced rapid time-dependent degradation of IκB-α and stimulated the phosphorylation of the NF-κB subunit p65/RelA (phosphorylated p65; Fig. 2 B). The time-dependent degradation of IκB-α and phosphorylation of the

NF-κB subunit p65/RelA (phosphorylated p65) caused by LPS was no longer observed in the presence of dDAVP (Fig. 2 B). Experiments using mpkCCD_{cl4} cells confirmed that dDAVP induced a dose-dependent decrease of the LPS-induced activation of NF-κB (Fig. 2 C). Consistent with these findings, dDAVP caused dose-dependent inhibition of LPS-stimulated secretion of MIP-2 and TNF-α (Fig. 2 D). A constant concentration of $10^{-8}$ M dDAVP also transactivated NF-κB and stimulated the secretion of MIP-2, and TNF-α inhibited to the same extent at all concentrations of LPS tested (Fig. 2, E and F), indicating that dDAVP does not bind to LPS in solution. To confirm that the inhibitory action of dDAVP on LPS-mediated cell activation involved the binding of dDAVP to V2R, the production of MIP-2 was
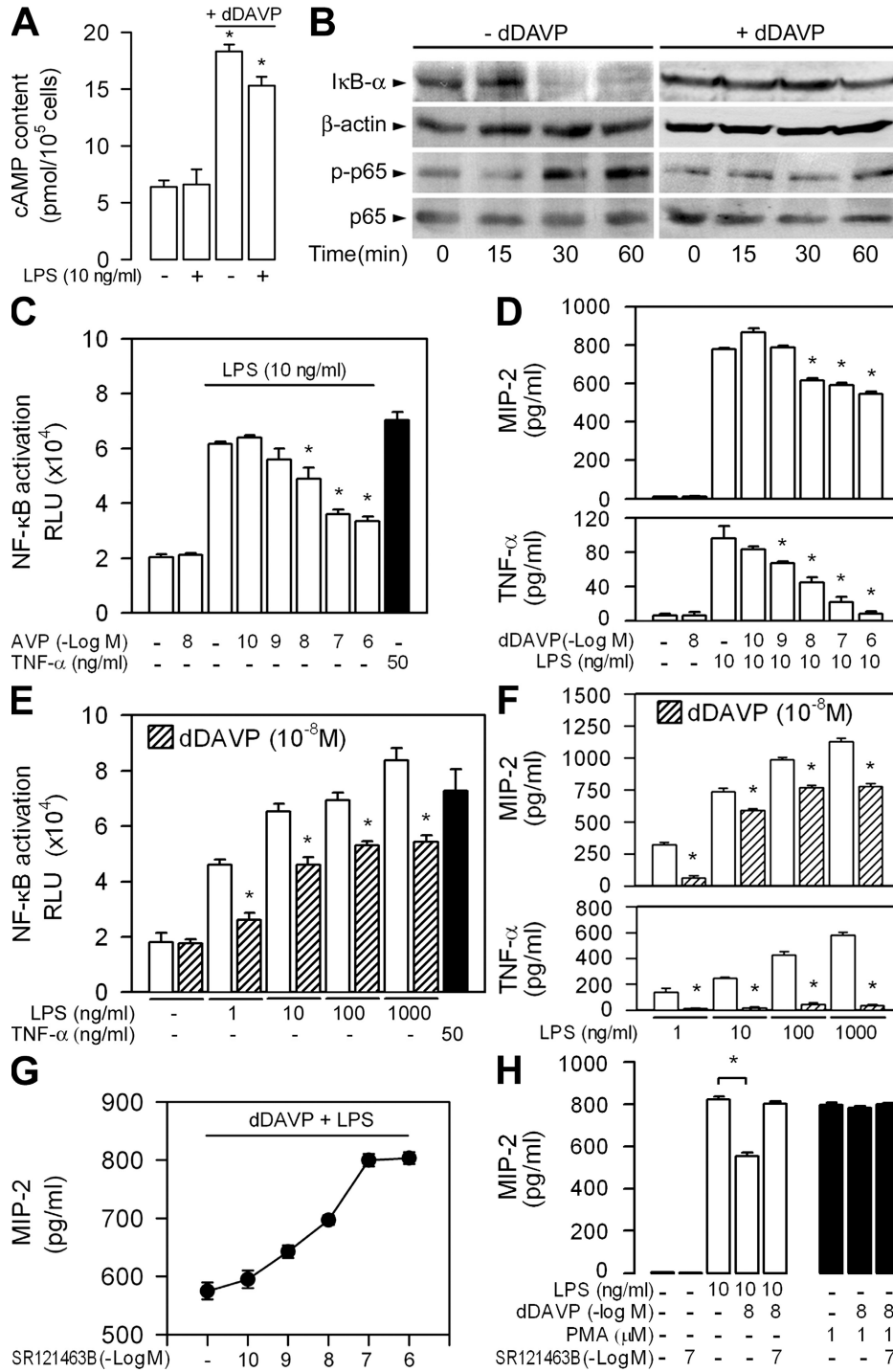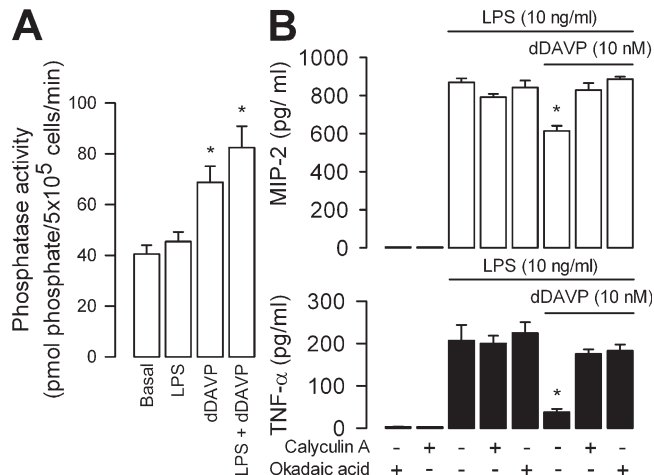
**Figure 2. Inhibitory effect of dDAVP on LPS–mediated cellular activation.** (A) Cell cAMP content in mpkCCD$_{cl4}$ cells incubated without or with $10^{-8}$ M dDAVP, LPS, or dDAVP plus LPS for 6 h. (B) Time-dependent expression of IκB-α and β-actin and phosphorylated (p-p65) and total (p65) NF-κB p65/RelA in cells incubated with LPS (−dDAVP) or LPS plus dDAVP (+dDAVP). (C and D) Effects of rising concentrations of dDAVP on 10 ng/ml LPS–induced cellular activation in mpkCCD$_{cl4}$ cells transfected with the NF-κB luciferase reporter (C), and on the secretion of MIP-2 and TNF-α (D). (E and F) Effects of $10^{-8}$ M dDAVP on 1–1,000 ng/ml LPS–induced cellular activation (E), and on the secretion of MIP-2 and TNF-α (F). TNF-α was used as control for the transactivation experiments. (G and H) Effects of SR121463B on the secretion of MIP-2 6 h after adding dDAVP and LPS. dDAVP and SR121463B had no effect on MIP-2 secretion stimulated by PMA. Results are expressed as means ± SE. *, P < 0.05 versus LPS values.

measured in mpkCCD$_{cl4}$ cells preincubated with increasing concentrations of SR121463B (see Materials and methods), a selective, nonpeptide V2R antagonist (31). Stimulations were subsequently performed with 10 ng/ml LPS plus $10^{-8}$ M dDAVP. SR121463B produced concentration-dependent antagonism of the inhibitory action of dDAVP on LPS-induced MIP-2 secretion: at $10^{-7}$ M, SR121463B completely antagonized the inhibitory action of dDAVP and restored the stimulatory activity of LPS (Fig. 2 G). The V2R-mediated inhibitory action of dDAVP appeared to be specific because neither dDAVP alone nor dDAVP plus SR121463B affected PMA-induced cell stimulation (Fig. 2 H). We then checked that dDAVP was acting specifically on the TLR4-mediated cellular activation. Extinction of TLR4 mRNA expression by a specific TLR4 small-interfering RNA (siRNA) completely inhibited the secretion of MIP-2 stimulated by LPS in mpkCCD$_{cl4}$ cells, whereas a negative control siRNA had no effect (Fig. S2, available at http://www.jem.org/cgi/content/full/jem.20071032/DC1). As a control, TLR4 extinction induced by the siRNA used had no effect on PMA stimulation. Involvement of PKA in the inhibitory action of dDAVP on LPS activation was demonstrated by preincubating the cells for 30 min with $5 \times 10^{-5}$ M of the selective PKA inhibitor H89. H89 significantly reduced the inhibitory effect of dDAVP on the LPS-mediated secretion of MIP-2 (LPS + dDAVP = 429 ± 31 pg/ml; LPS + dDAVP + H89 = 616 ± 11 pg/ml; $n = 4$; P < 0.05). In contrast, preincubating cells with $10^{-6}$ M GF109203X, a protein kinase C inhibitor, did not affect the inhibitory action of dDAVP on the LPS-mediated secretion of MIP-2 (LPS + dDAVP = 495 ± 17 pg/ml; LPS + dDAVP + GF109203X = 503 ± 18 pg/ml; $n = 4$). Collectively, these findings indicate that dDAVP acts as a potent modulator of the TLR4-dependent activation of renal CCD cells.

## The inhibitory effect of dDAVP on the LPS-induced secretion of MIP-2 and TNF-α is mediated by Ser/Thr protein phosphatases

dDAVP-induced down-regulation of LPS-mediated NF-κB activation suggests that this polypeptide hormone may alter the activation (i.e., phosphorylation) of signaling molecules. The phosphorylation of signaling molecules is regulated not only by protein kinases, but also by Ser/Thr protein phosphatases (32). PP1 and PP2A, as well as a variety of protein kinases, are involved in the regulation of signaling pathways by a phosphorylation/dephosphorylation mechanism (32). Interestingly, Ser/Thr PP2A is highly expressed in the distal nephron (33) and is activated by dDAVP in mouse renal collecting duct cells (34). We therefore investigated whether dDAVP activated Ser/Thr protein phosphatase activity, and whether calyculin A and okadaic acid, two potent inhibitors of Ser/Thr PP1 and PP2A (35), impaired the inhibitory effect of dDAVP on LPS-mediated cell stimulation. Incubating mpkCCD$_{cl4}$ cells with $10^{-8}$ M dDAVP for 6 h significantly stimulated PP2A activity (Fig. 3 A). 10 ng/ml LPS for 6 h also slightly increased the PP2A activity stimulated by dDAVP (Fig. 3 A).



**Figure 3.** Inhibitors of Ser/Thr protein phosphatases impair the inhibitory effect of dDAVP on the LPS-mediated cytokine secretion. (A) mpkCCD$_{cl4}$ cells were incubated with or without $10^{-8}$ M dDAVP, 10 ng/ml LPS, or dDAVP plus LPS for 6 h. Ser/Thr phosphatase activity was measured in cell homogenates using a synthetic phosphopeptide substrate. Error bars represent the mean phosphate release values ± SE from six separate experiments. (B) The secretion of MIP-2 and TNF-α was measured in the cell supernatants after incubation with or without 10 ng/ml LPS or $10^{-8}$ M dDAVP plus LPS for 6 h in the presence or absence of 10 nM calyculin A or okadaic acid. Values are means ± SE from four to seven separate experiments. *, P < 0.05 versus basal and LPS values (A) or versus the other experimental conditions (B).

In the absence of dDAVP, preincubating the cells with 10 nM calyculin A or okadaic acid had no effect on LPS-stimulated secretion of MIP-2 or TNF-α (Fig. 3 B). In sharp contrast, the two protein phosphatase inhibitors prevented the inhibitory effect of dDAVP on the LPS-stimulated secretion of MIP-2 and TNF-α (Fig. 3 B). Although calyculin A and okadaic acid both inhibit PP1 and PP2A activities, the latter is a more selective inhibitor of PP2A at the 10-nM dose used (36, 37). 10 nM calyculin A and okadaic acid also impaired the inhibitory effect of $10^{-8}$ M dDAVP on the stimulated secretion of MIP-2 and TNF-α at all concentrations of LPS (1–1,000 ng/ml) tested (Fig. S3, available at http://www.jem.org/cgi/content/full/jem.20071032/DC1). These findings strongly suggest that the increase in PP2A activity is directly responsible for the inhibitory effect of dDAVP on the LPS-stimulated secretion of both MIP-2 and TNF-α by renal collecting duct cells.

## Cl⁻ channel inhibitors abolish the inhibitory activity of dDAVP on LPS-stimulated cytokine secretion

CFTR, a Cl⁻ channel activated by cAMP-dependent PKA, can be dephosphorylated and inactivated by several Ser/Thr protein phosphatases (38–41). CFTR mediates the electrogenic apical secretion of Cl⁻ stimulated by dDAVP in renal collecting duct cells (12, 13). mpkCCD$_{cl4}$ cells express both ENaC and the CFTR Cl⁻ channel (Fig. 4 A). Two recent studies have demonstrated that the CFTR Cl⁻ channel is directly linked to PP2A (42, 43). Inhibitors of PP2A were also shown to prolong the deactivation of cAMP-activated CFTR
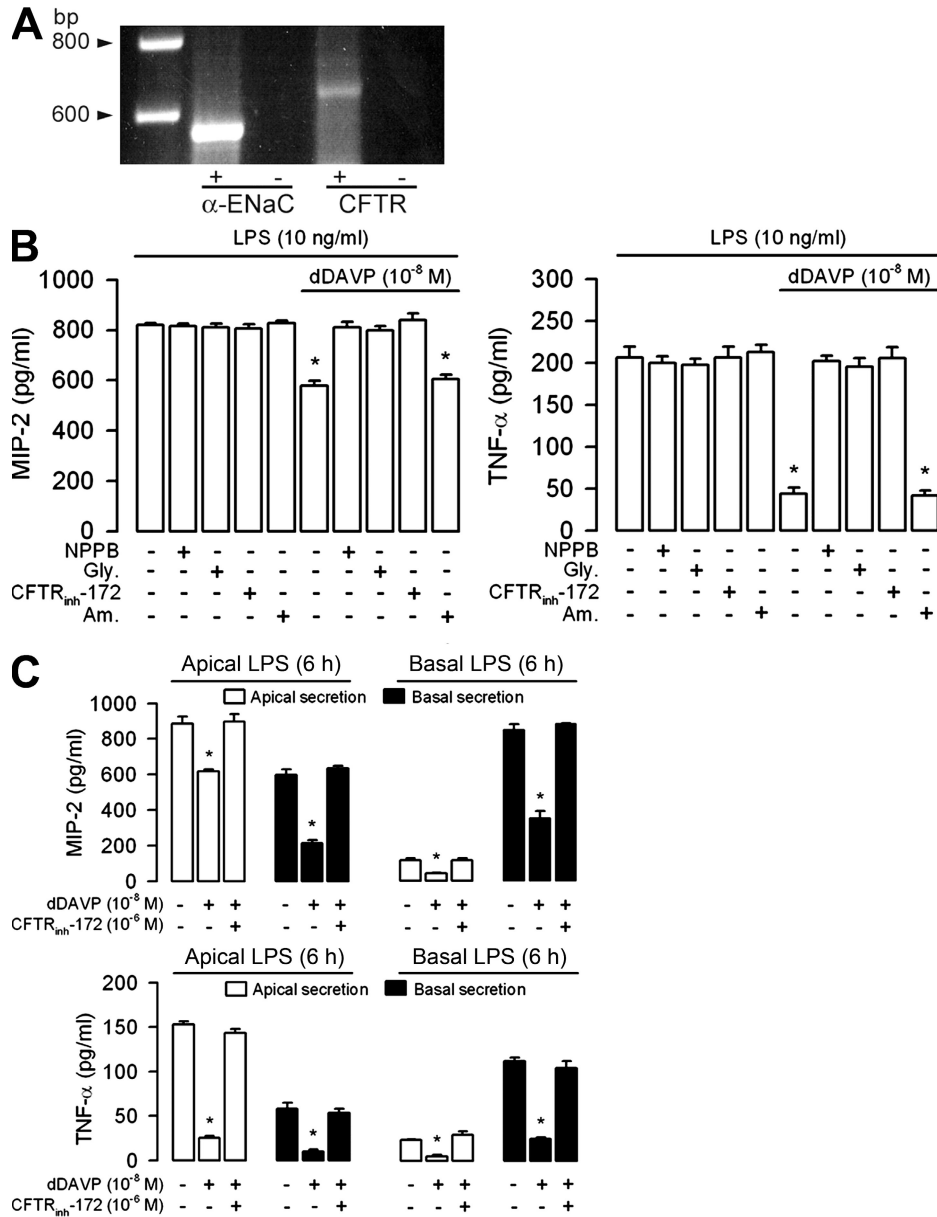
**Figure 4.   Anion channel inhibitors prevent the inhibitory effect of dDAVP on LPS–mediated cytokine secretion.** (A) mpkCCD$_{cl4}$ cells expressed α-ENaC (564 bp) and CFTR (636 bp) mRNA. + represents reverse-transcribed RNA; − represents non–reverse-transcribed RNA. (B) MIP-2 and TNF-α secretions were measured after incubating cells with or without 10 ng/ml LPS, 10$^{-8}$ M dDAVP, or dDAVP plus LPS for 6 h in the presence or absence of 10$^{-4}$ M NPPB, 10$^{-4}$ M Gly, 10$^{-7}$ M CFTR$_{inh}$–172, or 10$^{-5}$ M amiloride (Am). (C) Apical and basal secretion of MIP-2 and TNF-α measured on confluent cells grown on filters and incubated with 10 ng/ml LPS, LPS plus 10$^{-8}$ M dDAVP, or LPS plus dDAVP and 10$^{-7}$ M CFTR$_{inh}$–172. LPS was added either on the apical (Apical LPS) or basal (Basal LPS) side of the cell layers, dDAVP was added to the basal side of the cell layers, and CFTR$_{inh}$–172 was added to the apical side of the cell layers. Values are means ± SE from five to eight experiments (B) and from 7 to 10 measurements from three independent experiments (C). *, P < 0.05 versus LPS plus dDAVP values and the other experimental conditions.

Cl$^-$ channels in colonic carcinoma Caco-2 cells (42) and to increase CFTR channel activity in excised patches of airway and intestinal epithelium (43). Although protein phosphatase inhibitors had no substantial effects on dDAVP-stimulated Cl$^-$ fluxes in mpkCCD$_{cl4}$ cells (unpublished data), we wanted to find out whether CFTR was involved in the observed PP2A-dependent inhibitory effect of dDAVP on LPS-mediated

cell activation. We therefore tested the effects of various Cl$^-$ channel inhibitors on mpkCCD$_{cl4}$ cells exposed to LPS alone or to LPS plus dDAVP for 6 h (Fig. 4 B). 5–nitro-2(3phenyl-propyl-amino)benzoate (NPPB) and glybenclamide (Gly) both inhibit mouse CFTR at high concentrations and also affect other Cl$^-$ transporters, as well as K$^+$–ATP–sensitive channels (13, 44–46). The more potent and specific CFTR inhibitor

CFTR$_{inh}$–172 (see Materials and methods) was therefore also included in the analysis (47). $10^{-4}$ M NPPB and Gly significantly impaired the inhibitory activity of dDAVP on LPS-mediated secretions of MIP-2 and TNF-$\alpha$, whereas $10^{-5}$ M amiloride, a potent inhibitor of ENaC, did not affect cytokine secretion (Fig. 4 B). Importantly, $10^{-7}$ M CFTR$_{inh}$–172 also significantly diminished the inhibitory effect of dDAVP on the LPS-mediated secretion of MIP-2 and TNF-$\alpha$ (Fig. 4 B). Similar to what has been reported for calyculin A and okadaic acid, $10^{-7}$ M CFTR$_{inh}$–172 completely impaired the inhibitory effect of $10^{-8}$ M dDAVP on the stimulation of the secretion of MIP-2 and TNF-$\alpha$ at all concentrations of LPS (1–1,000 ng/ml) tested (Fig. S3).

Confluent mpkCCD$_{cl4}$ cells exhibit a highly differentiated, tight epithelial phenotype when grown on semipermeable filters and develop high transepithelial electrical resistance (>1,500 $\Omega$.cm$^2$) (21). The polarized (apical and/or basal) secretion of MIP-2 was measured in the apical and basal medium bathing confluent mpkCCD$_{cl4}$ cells grown on filters after being exposed to 10 ng/ml LPS for 6 h. Apical addition of LPS resulted in an increase in predominantly apically directed secretion of MIP-2 (Fig. 4 C). In contrast, basal addition of LPS induced only a moderate increase in the secretion of MIP-2, which appeared to be predominantly basally directed (Fig. 4 C). These findings demonstrate the presence of a predominantly apically oriented mechanism of LPS recognition and chemokine secretion in mpkCCD$_{cl4}$ cells. Similarly, apical addition of $10^{-7}$ M CFTR$_{inh}$–172 restored the LPS-stimulated apical and basal secretion of MIP-2 and TNF-$\alpha$ after the apical or basal addition of LPS to confluent cultures of dDAVP-treated mpkCCD$_{cl4}$ cells grown on filters (Fig. 4 C). These findings indicate that the cAMP-regulated CFTR Cl$^-$ channel, together with PP1 and PP2A, is involved in regulating the bipolarized cytokine secretion induced by LPS in renal collecting duct cells.

### The inhibitory effect of dDAVP on LPS–stimulated cytokine secretion requires intact CFTR

To assess further the role of CFTR in the down-regulation of the LPS-induced inflammatory responses elicited by dDAVP, experiments were performed using primary cultures of CCDs dissected from $cftr^{m1unc}$ and wild-type counterpart mice (hereafter referred to as $cftr^{+/+}$ and $cftr^{-/-}$ CCDs, respectively). Cultured $cftr^{+/+}$ and $cftr^{-/-}$ CCDs formed confluent layers of cuboid-shaped cells expressing K$_8$–K$_{18}$ cytokeratins and the tight junction–associated protein ZO-1 (Fig. 5 A). These cell layers were devoid of hematopoietic cells and did not express the bone marrow–derived cell marker CD45 (Fig. 5 B). $cftr^{+/+}$ and $cftr^{-/-}$ CCDs both expressed TLR4, whereas the expected size of CFTR transcripts was only observed in $cftr^{+/+}$ and not in $cftr^{-/-}$ CCDs (Fig. 5 C). dDAVP impaired the LPS-induced activation of the phosphorylated NF-$\kappa$B subunit p65/RelA in $cftr^{+/+}$ CCDs (Fig. 5, D and E). As in mpkCCD$_{cl4}$ cells, the decrease in phosphorylated p65 caused by dDAVP was no longer detected in LPS-treated wild-type $cftr^{+/+}$ CCDs incubated with $10^{-7}$ M CFTR$_{inh}$–172, 10 nM okadaic acid, or

calyculin A (Fig. 5 D). In sharp contrast, $cftr^{-/-}$ CCDs were completely resistant to the effect of dDAVP (Fig. 5, D and E). In line with these findings, dDAVP significantly reduced the LPS-induced secretion of MIP-2 and TNF-$\alpha$ in $cftr^{+/+}$ but not in $cftr^{-/-}$ CCDs (Fig. 5 F). Moreover, calyculin A, okadaic acid, and CFTR$_{inh}$–172 had no effect on LPS-treated $cftr^{-/-}$ CCDs (Fig. 5 F). These findings indicate that the inhibitory activity of dDAVP requires functional CFTR to control the activity of the Ser/Thr protein phosphatases in renal collecting duct cells.

### dDAVP inhibits UPEC–induced secretion of MIP-2 and TNF-$\alpha$ in cultured CCDs

To study the dDAVP-mediated effect on LPS-induced cell activation in a biologically relevant context, confluent cultures of CCDs dissected from TLR4-defective C3H/HeJ mice and from TLR4-expressing C3H/HeN mice (hereafter referred to as $Lps^d$ and $Lps^n$ CCDs, respectively) were analyzed after exposure to UPECs (6). dDAVP inhibited the secretion of MIP-2 and TNF-$\alpha$ in $Lps^n$ CCDs after the addition of LPS or HT7 UPEC isolates (Fig. 6, A and B). In contrast, no detectable LPS or dDAVP-induced effect was noted in $Lps^d$ CCDs (Fig. 6 A). In line with a previous study, which had demonstrated that UPEC isolates also activate a TLR4-independent signaling pathway (6), we found that incubating $Lps^d$ CCDs with UPECs resulted in residual cell stimulation. However, the levels of MIP-2 and TNF-$\alpha$ secreted by $Lps^d$ CCDs reached only $\sim$50% of those for $Lps^n$ CCDs. Importantly, TLR4-independent cell activation was not affected by preincubating with dDAVP (Fig. 6 B). These findings demonstrate that the suppressor effect of dDAVP is limited to TLR4-mediated cell activation and suggest that it may well be of biological relevance during UPEC infection.

### dDAVP–induced inhibition of the TLR4–mediated innate host defense in response to UPECs leads to exacerbated kidney infection in vivo

Increased AVP plasma levels are found in a variety of pathophysiological situations associated with dehydration, such as severe renal infection or septic shock. The question arises of the extent that dDAVP influences renal inflammatory responses and bacterial clearance. To answer this question, either 1 ng/$\mu$l/h dDAVP or 1 $\mu$l/h isotonic saline was administered continuously to adult female $Lps^n$ and $Lps^d$ mice via an implanted osmotic pump while receiving normal water intake (see Materials and methods) (48). Untreated $Lps^n$ and $Lps^d$ mice were kept in metabolic cages before and after the implantation of the osmotic pumps filled with dDAVP to find out whether dDAVP had similar antidiuretic effects in both mouse strains. dDAVP administration induced similar reduction in urine volume in both mouse strains (Table S1, available at http://www.jem.org/cgi/content/full/jem.20071032/DC1). In accordance with these results, urine osmolality increased and plasma osmolality decreased in all HT7-infected mice treated with dDAVP but not in those given isotonic saline (Table S2). Moreover, the magnitude of
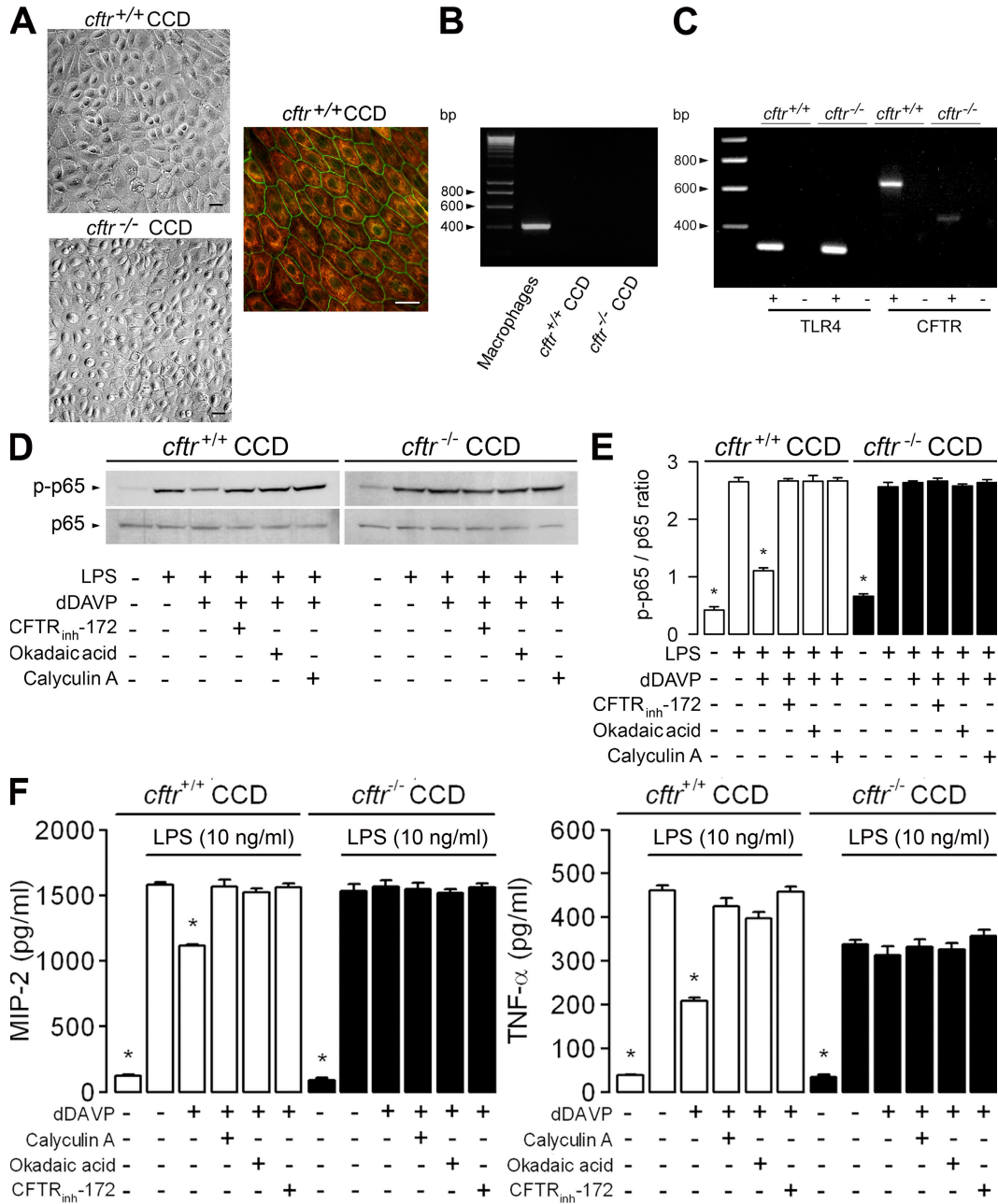
**Figure 5. The inhibitory effect of dDAVP on LPS–stimulated cytokine secretion requires functional CFTR.** (A) *cftr+/+* and *cftr−/−* CCDs formed confluent layers of cuboid cells and expressed cytokeratins 8–18 (red) and the tight junction–associated protein ZO-1 (green). Bars, 10 μm. (B) CD45 mRNA (405 bp) expressed in peritoneal macrophages was not detected in cultured *cftr+/+* CCDs. (C) Cultured *cftr+/+* CCDs and *cftr−/−* CCDs expressed TLR4 (311 bp) mRNAs. No amplified product of the expected size CFTR (636 bp) was detected in *cftr−/−* CCDs. + represents reverse-transcribed RNA; − represents non–reverse-transcribed RNA. (D) Western blots analyses of phosphorylated (p-p65) and total (p65) NF-κB p65/RelA after incubation of *cftr+/+* and *cftr−/−* CCDs with or without LPS or LPS plus dDAVP, and with or without CFTR$_{inh}$-172, okadaic acid, or calyculin A for 60 min (E). Error bars are the mean ratio values (arbitrary units) ± SE of densitometric analyses of phosphorylated over total p65 (*n* = 3) in the different conditions tested. (F) The secretion of MIP-2 was measured in *cftr+/+* CCD and *cftr−/−* CCD cell supernatants before and after adding LPS or LPS plus dDAVP with or without protein phosphatase and CFTR inhibitors for 6 h. Values are means ± SE from 7 to 11 wells from three to five separate experiments. *, P < 0.05 versus LPS plus dDAVP values and the other experimental conditions.

changes in plasma and urinary osmolalities reflecting the hydroosmotic activity of dDAVP were very similar in the *Lps^n* and *Lps^d* mice (Table S2). 24 h after the transurethral inoculation of the HT7 isolates, the expression of proinflammatory mediators and the renal bacterial burden were analyzed. The levels of IL-1β, MIP-2, regulated on activation,
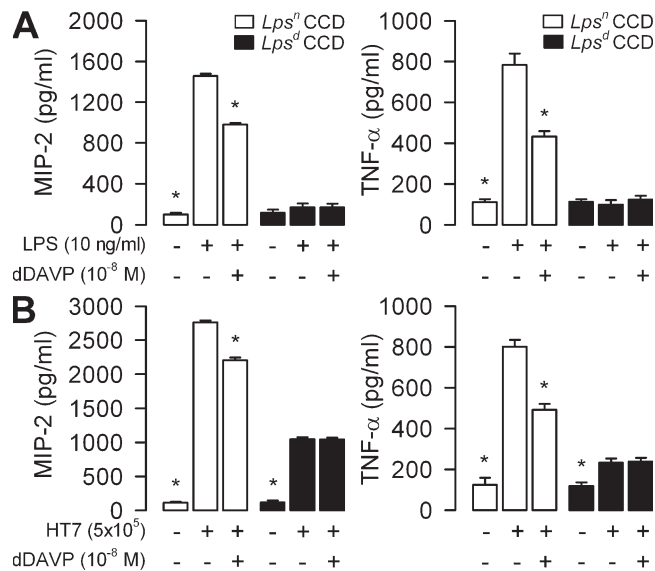
**Figure 6. Differential action of dDAVP on LPS- and UPEC-stimulated cytokine secretion in *Lps^n* and *Lps^d* CCD cells.** Secretion of MIP-2 and TNF-α was measured in confluent cultures of *Lps^n* and *Lps^d* CCDs incubated with LPS alone or LPS plus dDAVP for 6 h (A), or incubated with *E. coli* HT7 isolates ($5 \times 10^5$ bacteria per well) alone or HT7 plus dDAVP for 3 h (B). Values are means ± SE from five to seven separate wells from three separate experiments under each condition tested. *, P < 0.05 versus LPS or HT7 values (open bars) or HT7 and HT7 plus dDAVP values (shaded bars).

normal T cell expressed and secreted (RANTES), MCP-1, and TNF-α expression were lower in the dDAVP-treated *Lps^n* mice than in mice infused with isotonic saline after bacterial infection (Fig. 7 A). UPEC infection induced only a moderate increase in proinflammatory mediator expression in the kidneys of *Lps^d* mice, which was not altered by the dDAVP treatment (Fig. 7 A). dDAVP also dampened the production of MIP-2 and TNF-α measured in whole-cell homogenates from HT7-infected *Lps^n* mice but had no effect on the production of MIP-2 and TNF-α by HT7-infected kidneys of *Lps^d* mice (Fig. 7 B). These data are in accordance with the in vitro observations and further confirm that the suppressor effect of dDAVP is restricted to TLR4-dependent immune activation. The importance of TLR4 activation during UPEC infection was demonstrated by the finding that the renal bacterial burden was markedly greater in *Lps^d* than in *Lps^n* wild-type mice. Importantly, *Lps^n* mice treated with dDAVP were significantly more susceptible to UPEC infection than their *Lps^n* counterparts receiving isotonic saline, with a 20-fold greater bacterial CFU 1d after infection (Fig. 7 C). In contrast, dDAVP had no effect on the renal bacterial counts in *Lps^d* mice (Fig. 7 C).

Chemoattractant chemokines, such as MIP-2, play a key role in the migration of PMNs to mucosal sites of inflammation to produce efficient bacterial clearance (49, 50). In accordance with the lower expression of chemokines in infected *Lps^n* mouse kidneys treated with dDAVP, the number of Ly6-G–positive PMNs found on kidney sections from

infected mice 1d after bacterial challenge was significantly lower in dDAVP-treated *Lps^n* mouse kidneys than in the saline-infused *Lps^n* control mice (Fig. 7, D and E). In sharp contrast, the number of PMNs in UPEC-infected *Lps^d* kidneys, which was significantly lower than that in infected *Lps^n* mouse kidneys, was not affected by the dDAVP treatment (Fig. 7, D and E). The distribution of neutrophils in the pyelic and inner medullary regions of infected kidneys appears to be rather variable (Fig. 7 D). To confirm the immunohistological findings, neutrophil migration was also assessed by measuring myeloperoxydase (MPO) activity in renal homogenates (51). MPO assay revealed that neutrophil migration was lower in *Lps^d* than in *Lps^n* kidneys colonized by HT7 (Fig. 7 F). dDAVP infusion induced a marked decrease in MPO activity in the kidneys from HT7-infected *Lps^n* mice as compared with that of saline-infused infected *Lps^n* mice but had no effect on MPO activity in HT7-infected *Lps^d* kidneys (Fig. 7 F). These findings demonstrate that dDAVP also influences inflammatory responses in vivo and suggest that dDAVP may be involved during bacterial kidney infection. They also raised the question as to whether in vivo blockade of the endogenous V2R, which is highly expressed in collecting duct cells, could prevent the deleterious effect of dDAVP on the inflammatory response and bacterial burden. To answer this question, C3H/HeN *Lps^n* mice subjected to water restriction were given intraperitoneal injections of 0.03 or 0.3 mg/kg SR121463B 6 h before the transurethral inoculation of HT7. The mice received a second injection of SR121463B 14 h after bacterial infection. Administration of a low or high concentration of SR121463B alone had no effect on the levels of mRNA expression of proinflammatory mediators (Fig. 8 A). As a control, we checked that a high concentration ($10^{-6}$ M) of SR121463B did not affect the growth or viability of HT7 *E. coli* isolates (unpublished data). Also, the administration of low doses of SR121463B did not significantly affect plasma and urine osmolality (Table S3, available at http://www.jem.org/cgi/content/full/jem.20071032/DC1). Consistent with the decrease in urine osmolality caused by aquaresis (31), a high dose of the V2R antagonist (0.3 mg/kg) significantly increased plasma osmolality (Table S3). The administration of both low and high doses of SR121463B to infected mice resulted in significant dose-dependent increases in the expression of proinflammatory mediators and in the production of MIP-2 and TNF-α measured in whole kidney homogenates (Fig. 8, A and B). Compared with untreated infected mice, SR121463B treated mice also displayed a significant dose-dependent decrease in the renal bacterial burden 24 h after challenge (Fig. 8 C). Consistent with the stimulatory effect of the V2R antagonist on proinflammatory mediators, the number of CFU detected in kidneys proportionally decrease as a function of the dose of SR121463B administered (Fig. 8 C), whereas the number of Ly6-G–positive neutrophils infiltrating the kidneys and the levels of MPO activity remained almost the same in infected mice receiving a low dose (0.03 mg/kg) of SR121463B, and then fell significantly in infected mice treated with the high
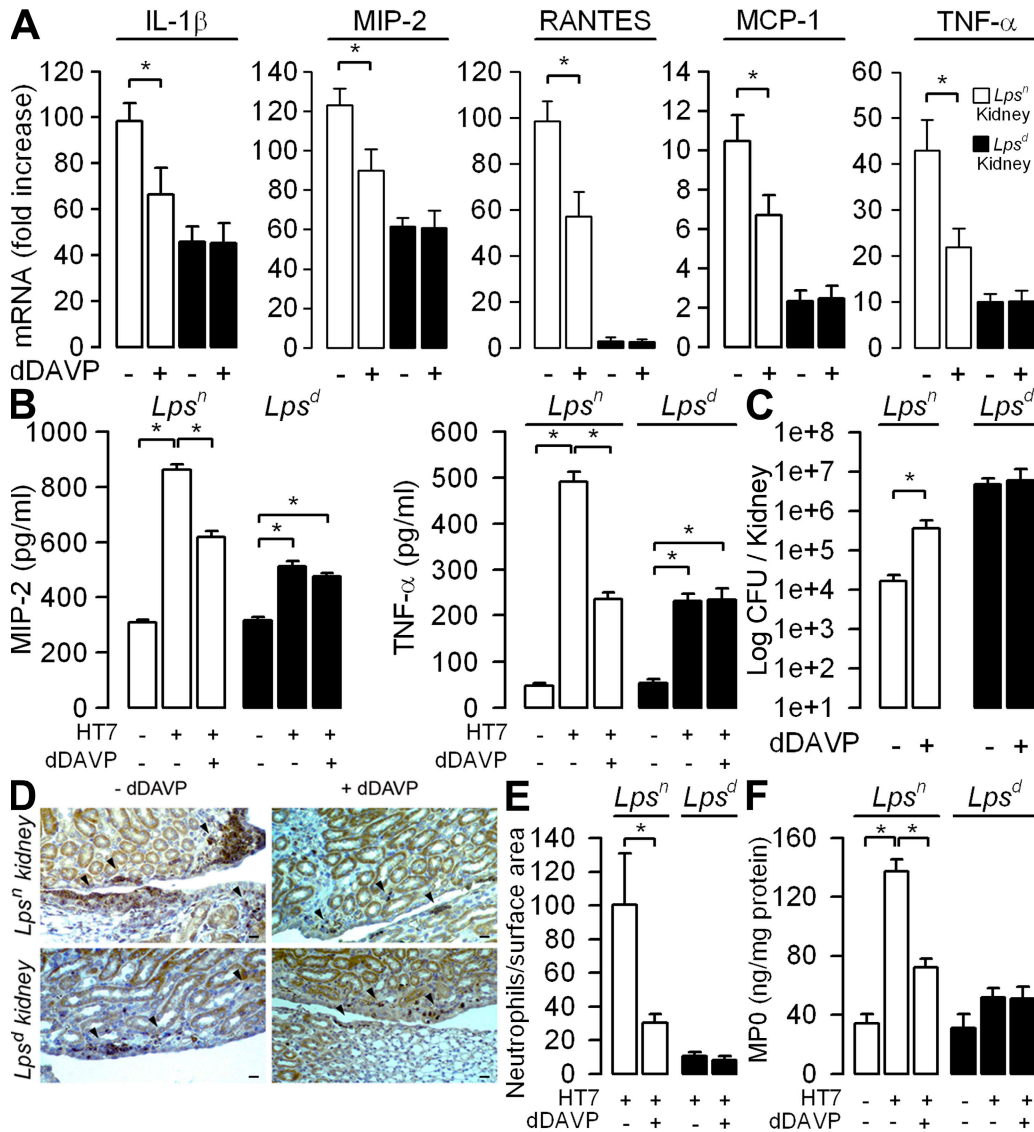
**Figure 7. Inhibitory action of dDAVP on inflammatory response, bacterial colonization, and neutrophil infiltrates in kidneys of mice challenged with UPECs.** dDAVP or isotonic saline was delivered via osmotic minipumps to $Lps^n$ and $Lps^d$ mice. Expression of proinflammatory mediators, production of cytokines, bacterial counts, numbers of infiltrating neutrophils, and MPO activity were determined in kidneys from isotonic saline control (−dDAVP) and dDAVP-treated (+dDAVP) $Lps^n$ (open bars) and $Lps^d$ (shaded bars) mice 24 h after the transurethral inoculation of HT7 isolates. (A) Relative fold increase of each mRNA level compared with that measured in naive mice. (B and C) Production of MIP-2 and TNF-α (B) and bacterial counts (C) in kidneys from HT7-infected $Lps^n$ and $Lps^d$ mice. (D and E) Illustrations (D) and quantification (E) of infiltrating Ly6-G–positive neutrophils (arrowheads) in kidney sections from HT7-infected $Lps^n$ and $Lps^d$ mice pretreated without (−dDAVP) or with dDAVP (+dDAVP). Bars, 50 µm. (F) Levels of MPO activity measured in kidney homogenates from uninfected and HT7-infected $Lps^n$ and $Lps^d$ kidneys treated or not with dDAVP. All values are means ± SE from measurements performed on six to eight different kidneys in each group tested. *, $P < 0.05$ between groups.

dose (0.3 mg/kg) of SR121463B (Fig. 8, D–F). Only a few UPECs (∼3,000 CFU per kidney) and infiltrating neutrophils were detected in kidneys from 0.3 mg/kg SR121463B–injected mice (Fig. 8, E and F). Furthermore, the small number of infiltrating neutrophils present in the infected kidneys from the 0.3 mg/kg SR121463B–injected mice was very similar to that found in dDAVP-treated $Lps^n$ mice, which exhibited ∼110-fold more bacteria in their kidneys (Fig. 7 D). These results suggest that SR121463B administration promoted

rapid renal clearance of bacteria by stimulating proinflammatory mediators. The beneficial effect of the V2R antagonist appeared to be restricted to the kidney, because the number of CFUs detected in the bladder did not considerably differ in untreated and SR121463B-treated mice (unpublished data). These findings support the idea that this potent V2R blocker agent, which may impair the retrograde ascent of UPECs via its aquaretic effects (31), effectively antagonizes the action of endogenous dDAVP, leading to a significant
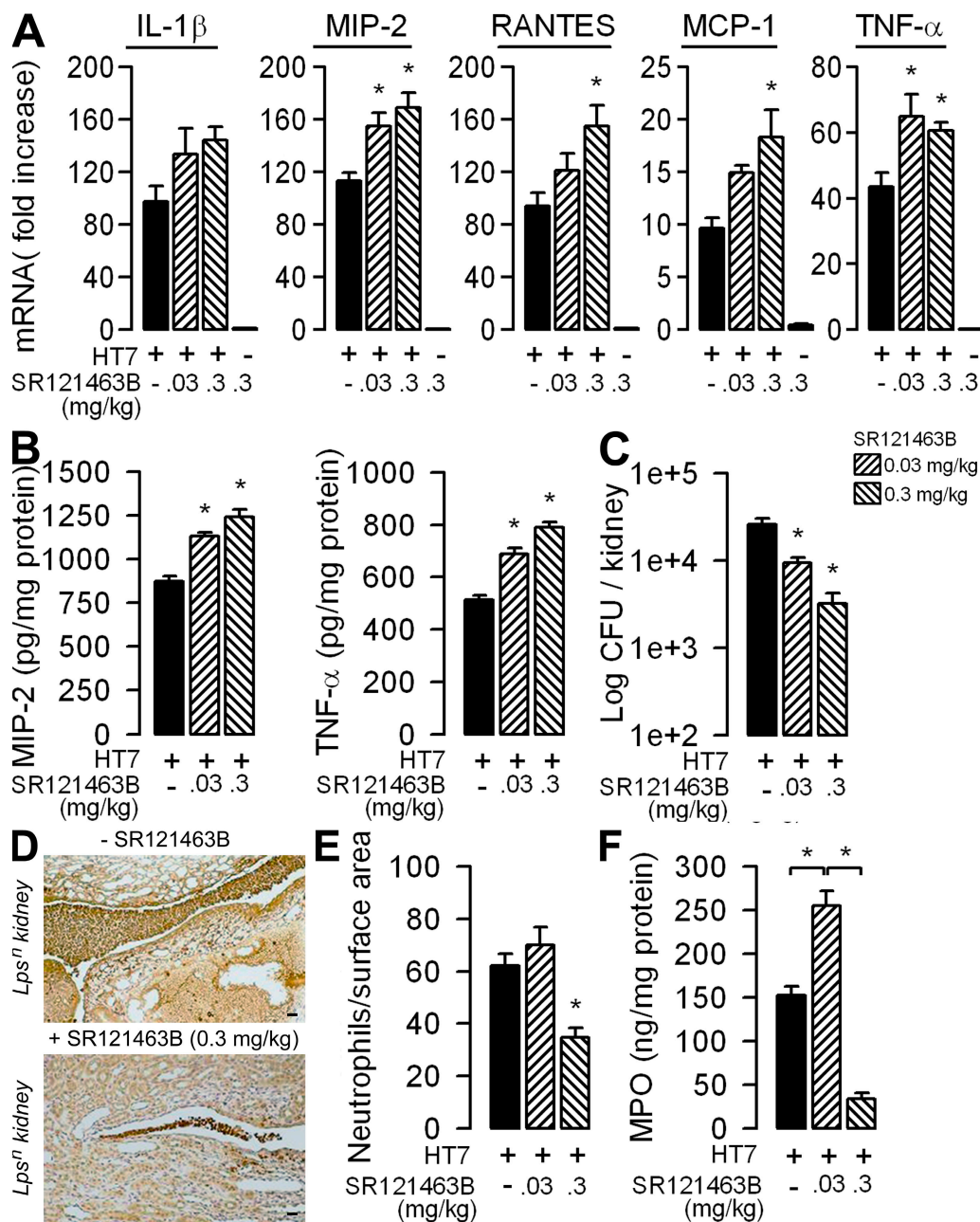
**Figure 8.** **The V2R antagonist SR121463B stimulates inflammatory response and promotes bacterial clearance in the kidneys of mice challenged with UPECs.** $Lps^n$ mice received intraperitoneal injections of SR121463B (0.03 or 0.3 mg/kg in 100 μl) 6 h before and after the transurethral inoculation of HT7 isolates. The expression of proinflammatory mediators, bacterial counts, numbers of infiltrating neutrophils, and MPO activity were performed 24 h after the transurethral inoculation of HT7 isolates. (A–C) Relative fold increase of each mRNA level of proinflammatory mediator compared with that measured in naive mice (A), production of MIP-2 and TNF-α (B), and bacterial counts (C) in kidneys from untreated and SR121463B-treated $Lps^n$ mice challenged with HT7. (D) Illustrations of neutrophil infiltrates (brown) in untreated (top), and 0.3 mg/kg SR121463B–treated (bottom) $Lps^n$ mice challenged with HT7. Bars, 50 μm. (E and F) Quantification of infiltrating neutrophils (E) and MPO activity (F) in kidneys from HT7-infected $Lps^n$ mice pretreated or not with SR121463B. All values are means ± SE from measurements performed on six to eight different kidneys in each group tested. *, $P < 0.05$ versus HT7 values and between groups.

(P < 0.05) increase in the expression of proinflammatory mediators and the subsequent activation of PMN influx, thereby promoting the recruitment of neutrophils to kill bacteria invading kidneys.

## DISCUSSION

Renal tubule collecting duct cells play an active role in initiating the inflammatory host defense during renal bacterial infection (6). In this paper, we show that the antidiuretic peptide AVP,

which acts on collecting duct cells, is also a potent immuno-modulator of the innate response elicited by UPECs. Previous studies have demonstrated that the stimulation of proinflam-matory responses in a variety of cell types is associated with down-regulation of cAMP and increased expression of intra-cellular adhesion molecule (ICAM) 1 (CD54) and vascular cell adhesion molecule 1, which are involved in the cell-to-cell contact–mediated host response (17, 52). In contrast, activa-tion of cAMP-mediated signaling may suppress the immune response elicited by LPS and TNF-α. Agents that increase cellular cAMP have also been shown to inhibit the TNF-induced expression of ICAM-1 and vascular cell adhesion molecule 1 in human lung epithelial A549 cells (52), airway smooth muscle cells (17), and activated macrophages (18, 19). In this study, dDAVP also inhibited the LPS-induced expres-sion of ICAM in mpkCCD$_{cl4}$ cells (unpublished data). A rise in cellular cAMP content was also shown to induce selective suppression of the activation of NF-κB in splenic B lympho-cytes by blocking the phosphorylation of NF-κB/RelA and the degradation of IκB-α (53). Similar to these previous findings, we show here that dDAVP inhibited both the LPS-induced degradation of IκB-α and its stimulation of phosphorylated p65/RelA, as well as LPS-mediated NF-κB activation and cytokine secretion in mpkCCD$_{cl4}$ cells. Ser/Thr protein phosphatases play key roles in the regulation of phosphoryl-ation of the NF-κB transcription factors. The SV40 small antigen, which associates with PP2A and inhibits its activity, enhances the activity of NF-κB (54). PP2A has been shown to dephosphorylate RelA directly in melanoma cell lines (55). In addition, the inhibition of PP1 and PP2A by okadaic acid induces the nuclear translocation and activation of NF-κB, as well as its activation in Jurkat cells and human neutro-phils (56, 57). We show that after specific binding to V2R, dDAVP stimulates PP2A activity in both untreated and LPS-treated mpkCCD$_{cl4}$ cells. These findings are consistent with those of a previous immunohistochemical study demon-strating that the expression of the PP2A protein is restricted to the epithelial cells of the distal nephron of adult rat and mouse kidneys (33, 34). We show that inhibition of PP2A activity by exposure to low concentrations of okadaic acid and calyculin A blunted the inhibitory effect of dDAVP on the LPS-stimulated secretion of MIP-2 and TNF. This suggests that the cAMP-dependent PKA activation caused by dDAVP leads to increased PP2A activity, which in turn inhibits IκB-α degradation and p65/RelA phosphorylation in renal collecting duct epithelial cells.

We also demonstrate that the inhibitory action of dDAVP on cellular activation requires an intact CFTR. The regula-tion of CFTR by PKA has been extensively studied. The regulatory domain (R domain) of CFTR harbors multiple consensus sites for phosphorylation by PKA. The phosphory-lation of the R domain regulates the opening of the CFTR channel (58). Multiple phosphatases may deactivate CFTR (38–41). PP2A has been shown to be one of the most potent protein phosphatases involved in the dephosphorylation of purified CFTR. Vastiau et al. (42) reported a direct and func-tional interaction between CFTR and PP2A. Using mass spectrometry, Thelin et al. (43) demonstrated that the PP2A catalytic A regulatory (Aα) and B′ (B′ε) regulatory subunits associate with CFTR, and that the latter binds directly to the C terminus of the CFTR molecule. PP2A inhibitors have also been shown to increase cAMP-stimulated CFTR currents in excised patches of airway epithelia and in intact mouse jejunum, and to delay their deactivation in colonic carcinoma Caco-2 cells (43, 44), which is consistent with physical inter-action between CFTR and PP2A. Although neither calyculin A nor okadaic acid had any effect on dDAVP-stimulated CFTR-mediated Cl⁻ secretion, they both impaired the in-hibitory effect of dDAVP on p65/RelA phosphorylation and on the secretion of MIP-2 and TNF-α elicited by LPS in mpkCCD$_{cl4}$ cells. CFTR blocking agents also impaired the inhibitory action of dDAVP on LPS-mediated activation. Collectively, these findings suggest that the closely associated CFTR and PP2A proteins are key signaling molecules activated by dDAVP, and that they down-regulate LPS-stimulated, TLR4-mediated inflammatory responses in renal collecting duct cells.

The cAMP-regulated CFTR is associated with inflam-matory processes in other cell types. For example, defective CFTR function is responsible for cystic fibrosis, a chronic inflammatory lung disease characterized by bacterial coloni-zation of the respiratory mucosa and an exaggerated and destructive chronic inflammatory response (59). CFTR has been shown to regulate the expression of RANTES, IL-8, IL-10, and inducible nitric oxide synthase (60). Interestingly, Estell et al. (60) also demonstrated that the CFTR-mediated NF-κB activation and RANTES expression require the insertion of CFTR into the plasma membrane. In this study, we show that the activation of the cAMP–PKA pathway by dDAVP, which down-regulates LPS-induced inflammatory responses in renal collecting duct cells, also requires an intact CFTR, which is inserted into the apical membrane of col-lecting duct cells in response to cAMP stimulation (12, 13). The inhibitory action of dDAVP seems to be restricted to the TLR4-mediated signaling pathway, because administration of the peptide hormone to mice infected by UPECs only altered inflammatory responses mediated by the TLR4 sig-naling cascade and not pathways independent of TLR4 (6). Our findings also suggest that activation of the PP2A–CFTR complex by dDAVP involves a dephosphorylation process on the TLR4-mediated, NF-κB signaling pathway. This sce-nario is consistent with a previous report showing that NF-κB activation and increased IL-8 production in cystic fibrosis tracheal epithelial cells is abrogated when dominant-negative signaling molecules, such as MyD88, are expressed (61).

Under conditions of dehydration, a rise in the circulatory level of vasopressin will stimulate NaCl and water reabsorp-tion from the terminal parts of the nephron. We show that AVP, via its stimulatory effect on CFTR and PP2A, simulta-neously reduces host inflammatory responses and favors renal bacterial invasion. This was illustrated by the fact that chronic administration of dDAVP reduces the renal expression of

proinflammatory mediators and the recruitment of PMNs, and increased the susceptibility of $Lps^n$ (but not $Lps^d$) mice to UPEC infection. The reduction in urine flow resulting from increased NaCl and water reabsorption may also contribute to the increased susceptibility to ascending bacterial infection. However, there is no reason why this effect should be restricted to $Lps^n$ mice.

It is generally agreed that adequate hydration helps to improve the resolution of UTIs and even to prevent them, although there is no direct clinical evidence that dehydration promotes UTIs in humans (62). However, previous experimental studies have demonstrated that water deprivation does considerably increase the risk of *E. coli*–induced pyelonephritis in rats (63) and that enterococcal-induced pyelonephritis in rats could be cured by sustained water diuresis (64). These studies are in accordance with the present findings showing that vasopressin impairs immune response both in vivo and in vitro. This means that it is conceivable that a sustained increased in the concentration of vasopressin in kidneys would tend to inhibit the local immune response and favor the bacterial colonization by ascending uropathogens. Such situations could account, at least in part, for the high frequency of UTI in elderly patients, who are particularly susceptible to dehydration.

The action of dDAVP in the down-regulation of inflammatory response observed in UPEC-infected kidneys has been confirmed by the blocking experiments using a V2R antagonist. Previous binding studies have demonstrated that nonpeptide V2R antagonists, including salts of SR121463 and Tolvaptan, display high competitive affinity for the renal V2R from different species, including mice and humans (31, 65, 66). These very selective compounds also display only very low affinity for other AVP receptor subtypes and do not bind to many of the receptors that are unrelated to AVP (65, 66). In in vivo studies, these V2R antagonists induce marked aquaresis in healthy and diseased animals, and clinical trials have shown that they improve hyponatremia, congestive heart failure, and various other diseases associated with volume overload (31, 66–68). Oral or intravenous administration of SR121463 salts induce dose-dependent aquaresis lasting 2–6 h (65). Unlike conventional diuretics, such as furosemide, the action of the SR121463 salts is purely aquaretic, with no major changes in urinary $Na^+$ or $K^+$ excretion (31). We show that blockade of V2Rs by SR121463B stimulated the expression of proinflammatory mediators in the kidneys of infected mice. Furthermore, the combination of the stimulated expression of proinflammatory mediators and aquaresis caused by high doses of SR121463B (0.3 mg/kg) resulted in the virtually complete clearance of UPECs colonizing the kidneys. These findings strongly suggest that in vivo, as in cultured collecting duct cells, dDAVP has a potent inhibitory effect on the inflammatory response in UPEC-infected kidneys.

To conclude, this study demonstrates that dDAVP, in addition to its key role in fluid homeostasis, also influences local innate immune recognition in the kidney by inhibiting TLR4-mediated cell activation in collecting duct epithelial cells. This pathway involves both PP2A and intact CFTR

$Cl^-$ channel activity. Importantly, the negative regulatory action of dDAVP described targets the site to which ascending uropathogenic *E. coli* preferentially adheres in vivo, and may therefore produce an important downstream effect on host defense activation, bacterial proliferation, and disease progression. Identification of this novel negative regulatory mechanism illustrates the important influence of hormonal control on local innate immune recognition and identifies a previously unrecognized factor of disease susceptibility and clinical outcome.

## MATERIALS AND METHODS

**Inhibitors.** NPPB was obtained from Research Biochemicals International. The thiazolidinone CFTR inhibitor 3-[(3-trifluoromethyl)phenyl]-5-[(4-carboxyphenyl)methylene]-2-thioxo-4-thiazolidinone ($CFTR_{inh}$-172) was provided by A.S. Verkman (University of California, San Francisco, San Francisco, CA). The V2R antagonist SR121463B (1-[4(N-tert-butylcarbamoyl)-2-methoxybenzene sulfonyl]-5-ethoxy-3-spiro-[4-(2-morpholinoethoxy) cyclohexane]indol-2-one, phosphate monohydrate) was provided by C. Serradeil-Le Gal (Sanofi-Aventis, Toulouse, France). SR121463B was dissolved in $10^{-2}$ M DMSO and then in 0.9% NaCl to produce the appropriate final concentration. PKA (H89) and PKC (GF109203X) inhibitors were obtained from Merck Biosciences. All reagents used were tested for the absence of LPS contamination using the *Limulus* amebocyte lysate assay (BioWhittaker).

**Mice, bacteria, and retrograde infection studies.** Adult female C3H/HeN ($Lps^n$) and C3H/HeJ ($Lps^d$) mice were obtained from the Jackson Laboratory. Homozygous mutant $cftr^{m1unc}$ ($cftr^{-/-}$) mice were obtained by a targeted mutation of the $cftr$ gene (23), and their wild-type counterpart ($cftr^{+/+}$) mice were obtained from the Centre de Développement des Techniques Avancées pour l'Expérimentation Animale (provided by M.F. Bertrand, Centre National de la Recherche Scientifique, Orléans, France). Mice originally derived from ES129/Sv cells injected into C57BL/6J mice embryos have been further backcrossed on a C57BL/6J background for three generations and were then intercrossed. All mice were housed under specific pathogen-free conditions and used when 8–13 wk of age. Renal retrograde UTI was performed on $Lps^n$ and $Lps^d$ mice, as previously described (6), using UPEC strain HT7. This UPEC strain was isolated from the urine of a woman with acute pyelonephritis and expresses the *pap* adhesin-encoding genes but lacks the *hly* α–hemolysin–encoding gene. The experimental procedures for the continuous infusion of dDAVP and administration of the V2R antagonist SR121463B before bacterial retrograde infection are listed in Supplemental materials and methods (available at http://www.jem.org/cgi/content/full/jem.20071032/DC1). The experiments were performed in accordance with the guidelines of the French Agricultural Office and in compliance with the legislation governing animal studies.

**Cell culture.** Experiments were performed on $mpkCCD_{cl4}$ cells (21) seeded on glass coverslips, Petri dishes, or Transwell permeable filters (0.4-μm pore size, 1-$cm^2$ insert growth area; Corning Costar Corp.) and on primary cultures of isolated CCDs microdissected from the kidneys of $Lps^n$ and $Lps^d$ mice, or from the kidneys of $cftr^{-/-}$ and $cftr^{+/+}$ mice, as previously described (6, 21). Cells were grown in a modified defined medium (DMEM/Ham's F12; 1:1 vol/vol; Invitrogen) supplemented with hormones and 2% fetal calf serum (21) in a 5% $CO_2$-95% air atmosphere. Confluent cells were incubated with purified *E. coli* (0111:B4 LPS Ultra-Pure; InvivoGen) or HT7 (5 × $10^5$ bacteria per well).

**Transient transfection and luciferase reporter assay.** 15 × $10^6$ $mpkCCD_{cl4}$ cells per milliliter were transfected by electroporation with the $p(\kappa B)_3$ IFN-Luc plasmid (a Luciferase cis-reporter system containing 7× AP-1 and 3× NF-κB enhancer elements), as previously described (69). Luciferase activity was measured with a luminometer using the Luciferase Assay System (Promega) according to the manufacturer's instructions.

**siRNA experiments.** The experimental procedure for TLR4 siRNA experiments is described in Supplemental materials and methods.

**Real–time and RT-PCR.** Total RNA was extracted from confluent whole kidneys or cultured CCD cells using the RNeasy mini kit (QIAGEN), according to the manufacturer's instructions, and reverse transcribed using Moloney murine leukemia virus reverse transcriptase (Invitrogen). cDNA was subjected to quantitative real-time PCR using a detector (Chromo 4; MJ Research). The mouse primers and TaqMan probes for IL-1β, MIP-2, MCP-1, RANTES, TNF-α, and β-actin were previously described (6). PCR data were reported as the relative increase in mRNA transcripts to that found in kidneys of naive mice or untreated cultured isolated CCDs, and were corrected by the respective levels of β-actin mRNA, which was used as the internal standard. cDNA and 400 ng of non–reverse-transcribed RNA were also subjected to RT-PCR using TLR4, MD-2, CD14, MyD88, α-ENaC, CFTR, or CD45 primers, as previously described (6).

**Histological and immunohistochemical studies.** Kidneys were fixed in Dubosc-Brazil solution, rinsed in PBS, embedded in paraffin, and stained with hematoxylin and eosin or periodic acid Schiff. Infiltrating PMNs were detected by immunohistochemical staining using an anti–Ly6-G (GR–1) antibody (1:1,000; BD Biosciences). The number of Ly6-G–labeled neutrophils per surface area ($10^4$ μm²) was counted on five different kidney tissue sections for each of the experimental conditions tested. Indirect immunofluorescence studies were performed as previously described (6) using an affinity-purified rabbit anti-TLR4 antiserum (1:100) (27), the mouse monoclonal CTR433 (provided by M. Bornens, Centre National de la Recherche Scientifique, Institut Curie, Paris, France), or the anti–NF-κB antibody (Santa Cruz Biotechnology Inc.). Cy3- and Alexa Fluor 488–conjugated IgG secondary antibodies were obtained from Jackson ImmunoResearch Laboratories. In some cases, nuclei were stained with Hoechst 33258 (Pierce Chemical Co). Specimens were examined using a confocal laser scanning microscope (510-META; Carl Zeiss MicroImaging, Inc.), and the images generated were photographed.

**FACS analysis.** TLR4/MD-2 intracellular staining was visualized using a rat monoclonal anti-TLR4/MD-2 (MTS510) antibody provided by K. Miyake (University of Tokyo, Tokyo, Japan) and a secondary goat anti–rat Cy5-conjugated antibody (Jackson ImmunoResearch Laboratories) after fixation (Cytofix; BD Biosciences) with or without permeabilization in $Ca^{2+}$, $Mg^{2+}$–free PBS containing 0.5% saponin and 2% FCS. Rat anti-hemagglutinin monoclonal antibody (Boehringer) was used as an isotype control.

**Western blotting.** Confluent cells were rinsed with PBS, scraped into 50 μl of lysis buffer (62.5 mM Tris-HCl [pH 6.8], 2% SDS, 10% glycerol, 50 mM DTT), and sonicated for 15 s at 4°C. Antibodies against TLR4 (27), IκB-α, total or phosphorylated NF-κB p65 (Cell Signaling Technology, Inc.), and β-actin (1:1,000; Sigma-Aldrich) were used to detect the corresponding antigens, as previously described (6).

**ELISA.** Cell supernatants from mpkCCD$_{cl4}$ cells or isolated CCDs in primary culture were collected, and the concentrations of MIP-2 and TNF-α were determined using DuoSet mouse MIP-2 and TNF-α ELISA kits (R&D Systems), according to the manufacturer's instructions. Kidneys from dDAVP- or SR121463B-treated $Lps^n$ and $Lps^d$ mice, some of which had been infected with HT7 isolates, were homogenized in 1 ml PBS and kept at −80°C until use. Tissue samples were thawed and assayed to measure the levels of MIP-2 and TNF-α production. Results were standardized to the amount of protein detected for each sample using a protein assay (Bio-Rad Laboratories) with BSA as standard. MPO activity was also measured using an ELISA kit (Hycult biotechnology), according to the manufacturer's instructions.

**Protein phosphatase assay.** PP2A activity was determined using a Ser/Thr phosphatase assay kit (Upstate Biotechnology), according to the directions supplied by the manufacturer.

**Cellular cAMP assay.** Confluent mpkCCD$_{cl4}$ cells were incubated with dDAVP, or with LPS or LPS plus dDAVP for 6 h. The cAMP content was measured using the cAMP Biotrak EIA system (GE Healthcare), according to the manufacturer's instructions.

**Statistics.** Results are expressed as means ± SE. Significant differences were analyzed using the unpaired Student's $t$ test and by analysis of variance using the Student-Newman-Keuls test and the Bonferroni $t$ test for multiple comparison procedures. $P < 0.05$ was considered significant.

**Online supplemental material.** Fig. S1 depicts the expression of TLR4 and associated signaling molecules in confluent mpkCCD$_{cl4}$ cells. Fig. S2 provides an illustration of mpkCCD$_{cl4}$ cells forming domes and the mRNA expression of TLR4 and associated signaling molecules. Fig. S3 illustrates the antagonist effect of Ser/Thr protein phosphatases and CFTR on the inhibitory action of dDAVP on LPS-mediated cytokine secretion. Table S1 summarizes the effects of dDAVP infusion on the volume of urine excreted by $Lps^n$ and $Lps^d$ mice housed in metabolic cages. Tables S2 and S3 show blood and urinary osmolality values 24 h after the inoculation of UPECs to untreated and dDAVP-treated mice or SR121463B-treated mice, respectively. Supplemental materials and methods provides information about the conditions of retrograde infection studies, dDAVP infusion, urine collection of mice acclimatized to metabolic cages, and administration of the V2R antagonist and TLR4 siRNA studies. Online supplemental material is available at http://www.jem.org/cgi/content/full/jem.20071032/DC1.

## REFERENCES

1. Brown, P., M. Ki, and B. Foxman. 2005. Acute pyelonephritis among adults: cost of illness and considerations for the economic evaluation of therapy. *Pharmacoeconomics*. 23:1123–1142.

2. Freedman, A.L. 2005. Urologic diseases in North America Project: trends in resource utilization for urinary tract infections in children. *J. Urol.* 173:949–954.

3. Pelle, G., S. Vimont, P.P. Levy, A. Hertig, N. Ouali, C. Chassin, G. Arlet, A. Rondeau, and A. Vandewalle. 2007. Acute pyelonephritis represents a risk factor impairing long-term kidney graft function. *Am. J. Transplant.* 7:899–907.

4. Poltorak, A., X. He, I. Smirnova, M.Y. Liu, C. Van Huffel, X. Du, D. Birdwell, E. Alejos, M. Silva, C. Galanos, et al. 1998. Defective LPS signaling in C3H/HeJ and C57BL/10ScCr mice: mutations in Tlr4 gene. *Science*. 282:2085–2088.

5. Hagberg, L., R. Hull, S. Hull, J.R. McGhee, S.M. Michalek, and C. Svanborg Eden. 1984. Difference in susceptibility to gram-negative urinary tract infection between C3H/HeJ and C3H/HeN mice. *Infect. Immun.* 46:839–844.

6. Chassin, C., J.M. Goujon, S. Darche, L. du Merle, M. Bens, F. Cluzeaud, C. Werts, E. Ogier-Denis, C. Le Bouguenec, D. Buzoni-Gatel, and A. Vandewalle. 2006. Renal collecting duct epithelial cells react to pyelonephritis-associated *Escherichia coli* by activating distinct

TLR4–dependent and –independent inflammatory pathways. *J. Immunol.* 177:4773–4784.

7. Fischer, H., M. Yamamoto, S. Akira, B. Beutler, and C. Svanborg. 2006. Mechanism of pathogen-specific TLR4 activation in the mucosa: fimbriae, recognition receptors and adaptor protein selection. *Eur. J. Immunol.* 36:267–277.

8. Schilling, J.D., S.M. Martin, C.S. Hung, R.G. Lorenz, and S.J. Hultgren. 2003. Toll-like receptor 4 on stromal and hematopoietic cells mediates innate resistance to uropathogenic *Escherichia coli*. *Proc. Natl. Acad. Sci. USA.* 100:4203–4208.

9. Patole, P.S., S. Schubert, K. Hildinger, S. Khandoga, A. Khandoga, S. Segerer, A. Henger, M. Kretzler, M. Werner, F. Krombach, et al. 2005. Toll-like receptor-4: renal cells and bone marrow cells signal for neutrophil recruitment during pyelonephritis. *Kidney Int.* 68:2582–2587.

10. Valenti, G., G. Procino, G. Tamma, M. Carmosino, and M. Svelto. 2005. Minireview: aquaporin 2 trafficking. *Endocrinology.* 146:5063–5070.

11. Bens, M., C. Chassin, and A. Vandewalle. 2006. Regulation of NaCl transport in the renal collecting duct: lessons from cultured cells. *Pflugers Arch.* 453:133–146.

12. Husted, R.F., K.A. Volk, R.D. Sigmund, and J.B. Stokes. 1995. Anion secretion by the inner medullary collecting duct. Evidence for involvement of the cystic fibrosis transmembrane conductance regulator. *J. Clin. Invest.* 95:644–650.

13. Bens, M., J.P. Van Huyen, F. Cluzeaud, J. Teulon, and A. Vandewalle. 2001. CFTR disruption impairs cAMP-dependent Cl− secretion in primary cultures of mouse cortical collecting ducts. *Am. J. Physiol. Renal Physiol.* 281:F434–F442.

14. Donald, R.A., R.R. Bailey, D. Hart, J.H. Livesey, M.J. Evans, L. Mattioli, J. Macdonald, and A.H. Smith. 1994. The plasma interleukin-6 and stress hormone responses to acute pyelonephritis. *J. Endocrinol. Invest.* 17:263–268.

15. Stattin Norinder, B., T. Sandberg, and R. Norrby. 2005. Renal concentrating capacity in female outpatients with symptomatic urinary tract infection. *Scand. J. Urol. Nephrol.* 39:483–487.

16. Rodionova, E.A., A.A. Kuznetsova, E.I. Shakhmatova, N. Prutskova, S. Nielsen, U. Holtback, Y. Natochin, and M. Zelenina. 2006. Urinary aquaporin-2 in children with acute pyelonephritis. *Pediatr. Nephrol.* 21:361–367.

17. Panettieri, R.A., Jr., A.I. Lazaar, E. Pure, and S.M. Albelda. 1995. Activation of cAMP-dependent pathways in human airway smooth muscle cells inhibits TNF-alpha–induced ICAM-1 and VCAM-1 expression and T lymphocyte adhesion. *J. Immunol.* 154:2358–2365.

18. Feng, W.G., Y.B. Wang, J.S. Zhang, X.Y. Wang, C.L. Li, and Z.L. Chang. 2002. cAMP elevators inhibit LPS-induced IL-12 p40 expression by interfering with phosphorylation of p38 MAPK in murine peritoneal macrophages. *Cell Res.* 12:331–337.

19. Osawa, Y., H.T. Lee, C.A. Hirshman, D. Xu, and C.W. Emala. 2006. Lipopolysaccharide-induced sensitization of adenylyl cyclase activity in murine macrophages. *Am. J. Physiol. Cell Physiol.* 290:C143–C151.

20. Aronoff, D.M., C. Canetti, C.H. Serezani, M. Luo, and M. Peters-Golden. 2005. Cutting edge: macrophage inhibition by cyclic AMP (cAMP): differential roles of protein kinase A and exchange protein directly activated by cAMP-1. *J. Immunol.* 174:595–599.

21. Bens, M., V. Vallet, F. Cluzeaud, L. Pascual-Letallec, A. Kahn, M.E. Rafestin-Oblin, B.C. Rossier, and A. Vandewalle. 1999. Corticosteroid-dependent sodium transport in a novel immortalized mouse collecting duct principal cell line. *J. Am. Soc. Nephrol.* 10:923–934.

22. Vinciguerra, M., U. Hasler, D. Mordasini, M. Roussel, M. Capovilla, E. Ogier-Denis, A. Vandewalle, P.Y. Martin, and E. Feraille. 2005. Cytokines and sodium induce protein kinase A-dependent cell-surface Na,K-ATPase recruitment via dissociation of NF-kappaB/IkappaB/protein kinase A catalytic subunit complex in collecting duct principal cells. *J. Am. Soc. Nephrol.* 16:2576–2585.

23. Snouwaert, J.N., K.K. Brigman, A.M. Latour, N.N. Malouf, R.C. Boucher, O. Smithies, and B.H. Koller. 1992. An animal model for cystic fibrosis made by gene targeting. *Science.* 257:1083–1088.

24. Jasmin, B.J., J. Cartaud, M. Bornens, and J.P. Changeux. 1989. Golgi apparatus in chick skeletal muscle: changes in its distribution during end

25. Guillot, L., S. Medjane, K. Le-Barillec, V. Balloy, C. Danel, M. Chignard, and M. Si-Tahar. 2004. Response of human pulmonary epithelial cells to lipopolysaccharide involves Toll-like receptor 4 (TLR4)-dependent signaling pathways: evidence for an intracellular compartmentalization of TLR4. *J. Biol. Chem.* 279:2712–2718.

26. Dunzendorfer, S., H.K. Lee, K. Soldau, and P.S. Tobias. 2004. Toll-like receptor 4 functions intracellularly in human coronary artery endothelial cells: roles of LBP and sCD14 in mediating LPS responses. *FASEB J.* 18:1117–1119.

27. Hornef, M.W., T. Frisan, A. Vandewalle, S. Normark, and A. Richter-Dahlfors. 2002. Toll-like receptor 4 resides in the Golgi apparatus and colocalizes with internalized lipopolysaccharide in intestinal epithelial cells. *J. Exp. Med.* 195:559–570.

28. Zhang, G., and S. Ghosh. 2001. Toll-like receptor-mediated NF-kappaB activation: a phylogenetically conserved paradigm in innate immunity. *J. Clin. Invest.* 107:13–19.

29. Baeuerle, P.A., and D. Baltimore. 1988. I kappa B: a specific inhibitor of the NF-kappa B transcription factor. *Science.* 242:540–546.

30. Brown, K., S. Gerstberger, L. Carlson, G. Franzoso, and U. Siebenlist. 1995. Control of I kappa B-alpha proteolysis by site-specific, signal-induced phosphorylation. *Science.* 267:1485–1488.

31. Serradeil-Le Gal, C. 2001. An overview of SR121463, a selective non-peptide vasopressin V(2) receptor antagonist. *Cardiovasc. Drug Rev.* 19:201–214.

32. Mumby, M.C., and G. Walter. 1993. Protein serine/threonine phosphatases: structure, regulation, and functions in cell growth. *Physiol. Rev.* 73:673–699.

33. Everett, A.D., C. Xue, and T. Stoops. 1999. Developmental expression of protein phosphatase 2A in the kidney. *J. Am. Soc. Nephrol.* 10:1737–1745.

34. Blot-Chabaud, M., N. Coutry, M. Laplace, J. Bonvalet, and N. Farman. 1996. Role of protein phosphatase in the regulation of Na+-K+-ATPase by vasopressin in the cortical collecting duct. *J. Membr. Biol.* 153:233–239.

35. Ishihara, H., B.L. Martin, D.L. Brautigan, H. Karaki, H. Ozaki, Y. Kato, N. Fusetani, S. Watabe, K. Hashimoto, and D. Uemura. 1989. Calyculin A and okadaic acid: inhibitors of protein phosphatase activity. *Biochem. Biophys. Res. Commun.* 159:871–877.

36. Takai, A., K. Sasaki, H. Nagai, G. Mieskes, M. Isobe, K. Isono, and T. Yasumoto. 1995. Inhibition of specific binding of okadaic acid to protein phosphatase 2A by microcystin-LR, calyculin-A and tautomycin: method of analysis of interactions of tight-binding ligands with target protein. *Biochem. J.* 306:657–665.

37. Favre, B., P. Turowski, and B.A. Hemmings. 1997. Differential inhibition and posttranslational modification of protein phosphatase 1 and 2A in MCF7 cells treated with calyculin-A, okadaic acid, and tautomycin. *J. Biol. Chem.* 272:13856–13863.

38. Hwang, T.C., M. Horie, and D.C. Gadsby. 1993. Functionally distinct phospho-forms underlie incremental activation of protein kinase-regulated Cl− conductance in mammalian heart. *J. Gen. Physiol.* 101:629–650.

39. Reddy, M.M., and P.M. Quinton. 1996. Deactivation of CFTR-Cl conductance by endogenous phosphatases in the native sweat duct. *Am. J. Physiol.* 270:C474–C480.

40. Travis, S.M., H.A. Berger, and M.J. Welsh. 1997. Protein phosphatase 2C dephosphorylates and inactivates cystic fibrosis transmembrane conductance regulator. *Proc. Natl. Acad. Sci. USA.* 94:11055–11060.

41. Luo, J., M.D. Pato, J.R. Riordan, and J.W. Hanrahan. 1998. Differential regulation of single CFTR channels by PP2C, PP2A, and other phosphatases. *Am. J. Physiol.* 274:C1397–C1410.

42. Vastiau, A., L. Cao, M. Jaspers, G. Owsianik, V. Janssens, H. Cuppens, J. Goris, B. Nilius, and J.J. Cassiman. 2005. Interaction of the protein phosphatase 2A with the regulatory domain of the cystic fibrosis transmembrane conductance regulator channel. *FEBS Lett.* 579:3392–3396.

43. Thelin, W.R., M. Kesimer, R. Tarran, S.M. Kreda, B.R. Grubb, J.K. Sheehan, M.J. Stutts, and S.L. Milgram. 2005. The cystic fibrosis transmembrane conductance regulator is regulated by a direct interaction with the protein phosphatase 2A. *J. Biol. Chem.* 280:41512–41520.

plate development and after denervation. *Proc. Natl. Acad. Sci. USA.* 86:7218–7222.

44. Schultz, B.D., A.K. Singh, D.C. Devor, and R.J. Bridges. 1999. Pharmacology of CFTR chloride channel activity. *Physiol. Rev.* 79:S109–S144.

45. Sheppard, D.N., and M.J. Welsh. 1992. Effect of ATP-sensitive K+ channel regulators on cystic fibrosis transmembrane conductance regulator chloride currents. *J. Gen. Physiol.* 100:573–591.

46. Rabe, A., J. Disser, and E. Fromter. 1995. Cl− channel inhibition by glibenclamide is not specific for the CFTR-type Cl− channel. *Pflugers Arch.* 429:659–662.

47. Ma, T., J.R. Thiagarajah, H. Yang, N.D. Sonawane, C. Folli, L.J. Galietta, and A.S. Verkman. 2002. Thiazolidinone CFTR inhibitor identified by high-throughput screening blocks cholera toxin–induced intestinal fluid secretion. *J. Clin. Invest.* 110:1651–1658.

48. Ge, Y., P.K. Stricklett, A.K. Hughes, M. Yanagisawa, and D.E. Kohan. 2005. Collecting duct-specific knockout of the endothelin A receptor alters renal vasopressin responsiveness, but not sodium excretion or blood pressure. *Am. J. Physiol. Renal Physiol.* 289:F692–F698.

49. Hang, L., M. Haraoka, W.W. Agace, H. Leffler, B. Burdick, R. Strieter, and C. Svanborg. 1999. Macrophage inflammatory protein-2 is required for neutrophil passage across the epithelial barrier of the infected urinary tract. *J. Immunol.* 162:3037–3044.

50. Frendeus, B., G. Godaly, L. Hang, D. Karpman, A.C. Lundstedt, and C. Svanborg. 2000. Interleukin 8 receptor deficiency confers susceptibility to acute experimental pyelonephritis and may have a human counterpart. *J. Exp. Med.* 192:881–890.

51. Rouschop, K.M., M. Sylva, G.H. Teske, I. Hoedemaeker, S.T. Pals, J.J. Weening, T. van der Poll, and S. Florquin. 2006. Urothelial CD44 facilitates *Escherichia coli* infection of the murine urinary tract. *J. Immunol.* 177:7225–7232.

52. Lee, J.H., L. Del Sorbo, S. Uhlig, G.A. Porro, T. Whitehead, S. Voglis, M. Liu, A.S. Slutsky, and H. Zhang. 2004. Intercellular adhesion molecule-1 mediates cellular cross-talk between parenchymal and immune cells after lipopolysaccharide neutralization. *J. Immunol.* 172:608–616.

53. Minguet, S., M. Huber, L. Rosenkranz, W.W. Schamel, M. Reth, and T. Brummer. 2005. Adenosine and cAMP are potent inhibitors of the NF-kappa B pathway downstream of immunoreceptors. *Eur. J. Immunol.* 35:31–41.

54. Sontag, E., J.M. Sontag, and A. Garcia. 1997. Protein phosphatase 2A is a critical regulator of protein kinase C zeta signaling targeted by SV40 small t to promote cell growth and NF-kappaB activation. *EMBO J.* 16:5662–5671.

55. Yang, J., G.H. Fan, B.E. Wadzinski, H. Sakurai, and A. Richmond. 2001. Protein phosphatase 2A interacts with and directly dephosphorylates RelA. *J. Biol. Chem.* 276:47828–47833.

56. Thevenin, C., S.J. Kim, P. Rieckmann, H. Fujiki, M.A. Norcross, M.B. Sporn, A.S. Fauci, and J.H. Kehrl. 1990. Induction of nuclear factor-kappa B and the human immunodeficiency virus long terminal repeat by okadaic acid, a specific inhibitor of phosphatases 1 and 2A. *New Biol.* 2:793–800.

57. Miskolci, V., S. Castro-Alcaraz, P. Nguyen, A. Vancura, D. Davidson, and I. Vancurova. 2003. Okadaic acid induces sustained activation of NFkappaB and degradation of the nuclear IkappaBalpha in human neutrophils. *Arch. Biochem. Biophys.* 417:44–52.

58. Gadsby, D.C., and A.C. Nairn. 1999. Control of CFTR channel gating by phosphorylation and nucleotide hydrolysis. *Physiol. Rev.* 79:S77–S107.

59. Machen, T.E. 2006. Innate immune response in CF airway epithelia: hyperinflammatory? *Am. J. Physiol. Cell Physiol.* 291:C218–C230.

60. Estell, K., G. Braunstein, T. Tucker, K. Varga, J.F. Collawn, and L.M. Schwiebert. 2003. Plasma membrane CFTR regulates RANTES expression via its C-terminal PDZ-interacting motif. *Mol. Cell. Biol.* 23:594–606.

61. Greene, C.M., T.P. Carroll, S.G. Smith, C.C. Taggart, J. Devaney, S. Griffin, S.J. O'neill, and N.G. McElvaney. 2005. TLR-induced inflammation in cystic fibrosis and non-cystic fibrosis airway epithelial cells. *J. Immunol.* 174:1638–1646.

62. Beetz, R. 2003. Mild dehydration: a risk factor of urinary tract infection? *Eur. J. Clin. Nutr.* 57(Suppl. 2):S52–S58.

63. Andriole, V.T. 1970. Water, acidosis and experimental pyelonepritis. *J. Clin. Invest.* 49:21–30.

64. Andriole, V.T., and J.P. Checko. 1968. Effect of water diuresis on chronic pyelonephritis. *J. Lab. Clin. Med.* 72:1–16.

65. Serradeil-Le Gal, C., C. Lacour, G. Valette, G. Garcia, L. Foulon, G. Galindo, L. Bankir, B. Pouzet, G. Guillon, C. Barberis, et al. 1996. Characterization of SR 121463A, a highly potent and selective, orally active vasopressin V2 receptor antagonist. *J. Clin. Invest.* 98:2729–2738.

66. Miyazaki, T., H. Fujiki, Y. Yamamura, S. Nakamura, and T. Mori. 2007. Tolvaptan, an orally active vasopressin v(2)-receptor antagonist-pharmacology and clinical trials. *Cardiovasc. Drug Rev.* 25:1–13.

67. Schrier, R.W., P. Gross, M. Gheorghiade, T. Berl, J.G. Verbalis, F.S. Czerwiec, and C. Orlandi, for the SALT Investigators. 2006. Tolvaptan, a selective oral vasopressin V2-receptor antagonist, for hyponatremia. *N. Engl. J. Med.* 355:2099–2112.

68. Gheorghiade, M., I. Niazi, J. Ouyang, F. Czerwiec, J. Kambayashi, M. Zampino, C. Orlandi, and Tolvaptan Investigators. 2003. Vasopressin V2-receptor blockade with tolvaptan in patients with chronic heart failure: results from a double-blind, randomized trial. *Circulation.* 107: 2690–2696.

69. Pedruzzi, E., C. Guichard, V. Ollivier, F. Driss, M. Fay, C. Prunet, J.C. Marie, C. Pouzet, M. Samadi, C. Elbim, et al. 2004. NAD(P)H oxidase Nox-4 mediates 7-ketocholesterol-induced endoplasmic reticulum stress and apoptosis in human aortic smooth muscle cells. *Mol. Cell. Biol.* 24:10703–10717.